

theories such as that from Marcus: reaction energetics, electronic couplings between states involved in the dynamics, and reorganization energies. Importantly, though, system specific and environment specific details that impact these parameters matter. For example, there need not be a unifying character in all dimers as to the nature of the reactant singlet. In some systems there is an expectation that it is single-chromophore localized within the dimer,^{11,12} while in other systems, a more delocalized exciton or even an excimer^{19,20,22,25,26,37} is expected given larger interchromophore Coulomb couplings. These issues will certainly impact photoreaction energies, reorganization energy, and likely as well, the $S_1/{}^1\text{TT}$ electronic coupling. As discussed more in this paper, this is a question we are interested in addressing for the types of dimers being synthesized and studied in our laboratory. In still other systems, the electronic nature of the reactant singlet can significantly alter along the initial reaction coordinate, for example, by taking on charge transfer (CT) character during interchromophore conformational changes.²⁵ This will impact reaction energetics and $S_1/{}^1\text{TT}$ electronic coupling.

As examples of more environment-specific perturbations to decay mechanism, it is worth highlighting recent dimer work that has spectroscopically characterized CT states. Such states are important in two general scenarios. In the first, which is most commonly discussed in a diabatic-state picture and referred to as mediated coupling, they can serve as virtual intermediates that enhance the electronic interaction between the S_1 photoreactant and the ${}^1\text{TT}$ photoproduct through second-order terms in the coupling expressions.^{4,15,40,41} Because the solvent is not expected to reorient during this coupling, its polarizability and not its polarity is key for affecting the relative importance of CT states.¹¹ In the second scenario, CT states serve as actual intermediates in the photoreaction pathway, causing polarity to take precedence over polarizability. However, this pathway may not involve ${}^1\text{TT}$: in the first observation by Johnson and co-workers studying 1,3-diphenylisobenzofuran dimers in polar DMSO, the ${}^1\text{CT}$ is formed from S_1 on a 150 to 250 ps time scale (depending on dimer).¹¹ Triplets are observed in these systems in low yield, although it is believed that they could come, not from ${}^1\text{TT}$, but from an ISC/IC pathway: ${}^1\text{CT} \rightarrow {}^3\text{CT} \rightarrow \text{T}_1$. Most of the excited-state population decays via back electron transfer (${}^1\text{CT} \rightarrow \text{S}_0$), and thus in these systems, the CT is serving as a trap state that undermines, rather than enhances, ${}^1\text{TT}$ formation. A similar situation is observed for a 7.6 Å slip-stacked terrylenediimide covalent dimer.²⁶ For that species in polar methylene chloride, a CT trap state is observed, and charge recombination serves as the dominant decay pathway. When that molecule is in nonpolar toluene, the CT state is virtual, and ${}^1\text{TT}$ formation is highly efficient. Finally, Lukman and co-workers also observe the ${}^1\text{CT}$ acting as a trap state in studies of (trialkylsilyl)acetylene-substituted 6,6'-dipentacenyl dimers in polar environments.²⁵ However, they argue that ${}^1\text{TT}$ is still formed in reasonable to high yield in polar environments (yield depending on the specific solvent polarity). This may suggest that they are tuning the energy of the ${}^1\text{CT}$ between the reactant S_1 and the ${}^1\text{TT}$, although as alluded to above, this may be an oversimplification if the electronic nature of the reactant singlet is significantly modified along the initial reaction coordinate.

Our interest in dimer systems was initiated by a mechanistic exploration, not of a molecular system, but of the tetracene molecular solid studied as a polycrystalline thin film using laser

pulse-shaping experiments.⁴² There we saw evidence that low-frequency intermolecular lattice vibrations modulate SF yields, and we argued that inter-acene motions mediated through π -systems could alter electronic coupling for the $S_1 \rightarrow {}^1\text{TT}$ photoreaction, thus giving it greater prominence relative to competing excited-state processes such as trap formation.⁴² These findings led us toward molecular dimer systems where, in principle, tools of synthesis could be exploited to control the relative spatial arrangement of chromophores.^{43,44} A partially cofacial and geometrically well-defined tetracene system called BT1 (see Figure 1) was studied with electronic structure

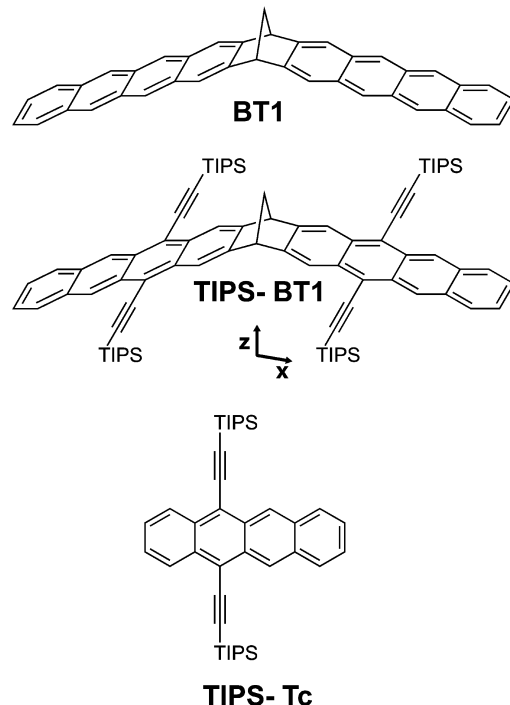


Figure 1. BT1 is a structurally well-defined bistetracene dimer previously studied by our group.^{12,15,21,31} TIPS-BT1 is the dimer studied herein along with the monomer model TIPS-Tc. The spatial orientation of TIPS-BT1 is indicated to aid in the discussion of electronic absorption polarizations.

theory,¹² theory related to vibronic coupling,¹⁵ and then synthesized³¹ and explored with static and time-resolved photoluminescence spectroscopies.²¹ The experimental findings are consistent with the theoretical predictions inasmuch as the $S_1 \rightarrow {}^1\text{TT}$ photoreaction is slow, particularly when compared to other tetracene dimer systems in the literature.²³ This can be understood because BT1 has considerable symmetry (C_{2v} point group in its ground-state geometry) and as long as a reflection plane passes through both chromophores of the dimer, the diabatic coupling for the initial photoreaction (e.g., $S_1\text{S}_0 \rightarrow {}^1\text{TT}$) is formally zero.^{15,16} Diabatic coupling can emerge through vibrations having specific symmetry properties^{15,16} but the dynamics measured with photoluminescence techniques suggest the magnitude remains small. Unfortunately, unfavorable solubility and stability of BT1 precluded extensive mechanistic exploration and spectral characterization using transient absorption tools, as is common for many dimer systems. As well, they precluded variation of solvent to increase polarity and polarizability to search for and explore the role of CT states implicated in the mechanism of SF.^{11,25,26}

In order to move forward with more detailed studies, we synthesized a related dimer system TIPS-BT1 (see Figure 1) bearing bulky triisopropylsilyl (TIPS) acetylene substituents that serve to enhance solubility and stability toward oxidation.³¹ (Trialkylsilyl)acetylene moieties of this nature have proven to be useful in pentacenic dimer systems reported by several groups.^{13,18,19,25,30,31} In the current work, we apply a suite of static and time-resolved spectroscopies including transient absorption to characterize the behavior of TIPS-BT1 relative to a monomeric model TIPS-Tc (see Figure 1). After an initial characterization with static spectroscopies in Part 1, these systems are studied (Part 2) in the nonpolar solvent toluene in order to draw connections with BT1.²¹ Interesting differences emerge that can be tied to state-energy perturbations due to the TIPS- acetylene substituents. In Part 3, the dynamics of TIPS-BT1 are explored in the polar solvent benzonitrile at room temperature and with variable temperature measurements. A detailed photophysical picture emerges, and there are two key findings. First, photoexcitation leads to separate populations of both arm-localized and delocalized singlet exciton states. Interestingly, these populations do not interconvert with each other once formed, and the arm-localized exciton decays directly to the ground state. Second, the delocalized exciton state equilibrates with a spectrally distinct intramolecular CT state on a 50 ps time scale. This excited-state equilibrium then decays to the ground state with no evidence for production of triplets. While ineffective at the $S_1 \rightarrow ^1\text{TT}$ photoreaction, the TIPS-BT1 system has excellent properties for characterization of states implicated in this process, thus benchmarking for future studies where electronic coupling and reaction energetics are engineered for a more facile reaction.^{16,31}

II. RESULTS AND DISCUSSION

Part 1. Initial Characterization with Static Spectroscopies. Electronic Absorption in Chloroform. Electronic absorption spectra of TIPS-Tc and TIPS-BT1³² are first compared in chloroform in order to preserve information in the UV that is cut off by solvent absorption in toluene and benzonitrile, which are used later to study dynamics. Spectra are shown in Figure 2 while tabulated data (Table S1) and detailed discussion about the assignment of features in terms of a simple transition dipole moment model (as was done for BT1 and a monomer model in previous work²¹) can be found in the Supporting Information (SI). In summary, there are two important observations in the dimer TIPS-BT1 relative to the

TIPS-Tc monomer model: first, the emergence of a split feature in the $S_3 \leftarrow S_0$ region (250–350 nm) and second, a near-doubling of the molar attenuation coefficient of a single vibronic progression in the $S_1 \leftarrow S_0$ region. The former, which is also seen in BT1 and in the bis-naphthalene dimer that inspired it, is a striking example of excitonic interaction and is attributed to Davydov-splitting originating from the Coulomb interaction between two chromophore-localized long-axis $S_3 \leftarrow S_0$ transitions.^{21,34,44} The latter is behavior consistent with two weakly coupled absorbing chromophore arms in an H- or J-aggregate⁴⁵ and has been observed by others.^{18,19,23,27,30,46} Because the $S_1 \leftarrow S_0$ transitions on each arm of TIPS-BT1 are short axis, their interaction is H-aggregate-like, leading to one dark pathway (a lower-energy, out-of-phase combination) and one bright pathway (the higher-energy, in-phase combination) with doubled intensity. This is the single vibronic progression observed between 450 and 550 nm. The assignment of weak coupling is further based on a 0–0 to 0–1 absorption ratio that is similar to that of the monomer but with some evident 0–0 peak suppression, consistent with a molecule in a weakly coupled H-aggregate (in the strong coupling limit the 0–0 transition would be completely suppressed).⁴⁷

Static Electronic Spectroscopy as Solvent Environment is Varied. Two solvent environments were chosen for exploration of time-resolved photophysics (vide infra). Toluene is nonpolar and offers a basis for comparison with our previous explorations of BT1.²¹ Benzonitrile is polar but has a polarizability that is comparable to toluene. Figure 3 shows steady-state absorption and emission of TIPS-Tc (blue) and TIPS-BT1 (red) as the chromophores are placed in nonpolar toluene and polar benzonitrile. Chloroform data are included for comparison. That solvent has polarity that is intermediate between toluene and benzonitrile, although the relative positions of empirical parameters used to quantify polarity are expected to vary depending on the types of chromophores used in measurement.⁴⁸

As in chloroform, electronic absorbance of the norbornyl-bridged TIPS-BT1 dimer (S_1 onset at 528 nm) is slightly blue-shifted relative to the TIPS-Tc monomer (S_1 onset at 535 nm) due to electronic destabilization from the bridge.¹² Both monomer and dimer experience subtle but measurable absorption solvatochromism in the form of a bathochromic shift when moving from toluene to the more polar benzonitrile (535 nm in the monomer becomes 539 nm, and 528 nm in the dimer becomes 532 nm). This observation is consistent with CT character⁴⁸ and with the current understanding of the S_1 in polyacenes for which this character has been described as “hidden”.⁴⁹ Excepting this solvatochromism, there are minimal changes in the structure of the electronic absorption of either molecule as solvent polarity is increased. We note that there is no observable absorption solvatochromism on going from toluene to chloroform even while polarity is expected to increase. At this point, we lack an explanation for this observation.

Moving to emission, it is again the case that there is a subtle ~5 nm bathochromic shift for both molecules as solvent is varied from nonpolar to polar. In all solvents, the monomer TIPS-Tc appears to emit from the same state based on the mirroring of absorption features. This is likewise the case for TIPS-BT1 in the nonpolar toluene. There are, on the other hand, notable changes in the breadth and overall shape of the TIPS-BT1 spectrum in benzonitrile. With these observations in hand, we will first explore the photophysical behavior of TIPS-

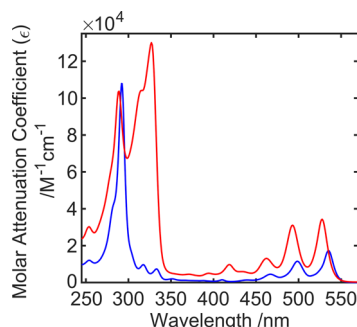


Figure 2. Electronic absorption spectra of TIPS-Tc (blue) and TIPS-BT1 (red) in CHCl_3 , showing features in the UV region. The bright two-peaked feature in the UV for TIPS-BT1 indicates Davydov splitting.

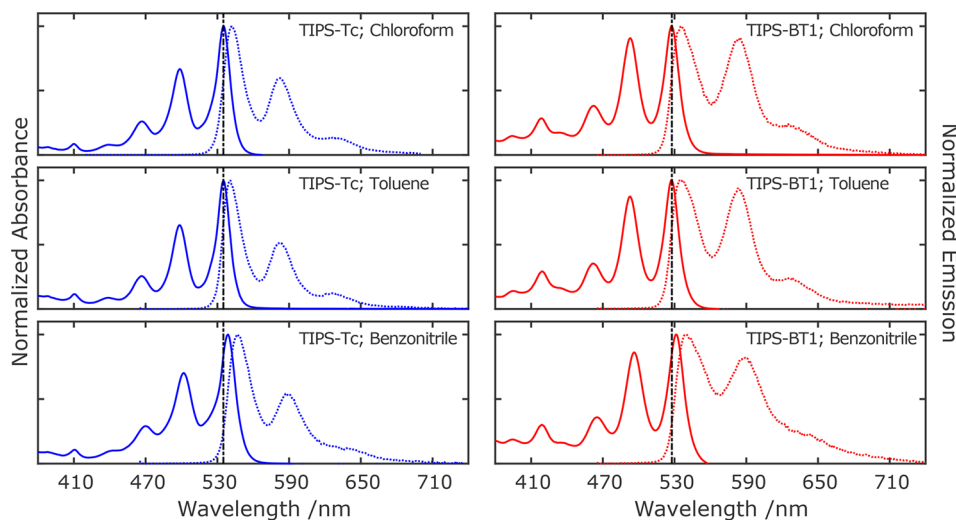


Figure 3. Room-temperature electronic absorption spectra (solid lines) and emission spectra (dashed lines) of monomer TIPS-Tc (blue) and dimer TIPS-BT1 (red) in chloroform (top), toluene (middle), and benzonitrile (bottom). Vertical dashed lines highlight the S_1 absorption onsets in the nonpolar solvents chloroform and toluene, showing slight solvatochromism with benzonitrile.

BT1 and TIPS-Tc in the nonpolar toluene environment. Following this, we return to benzonitrile with time-dependent measurements that help to explain the aforementioned emission spectral features seen in Figure 3 for TIPS-BT1.

Part 2. Excited State Dynamics in a Nonpolar Toluene Environment. *Photophysics in Toluene.* Photoluminescence quantum yields (Φ_{em}) and observed emission lifetimes were measured for TIPS-BT1 and TIPS-Tc (Table 1).

Table 1. Summary of Room-Temperature Photoluminescence Behavior for Monomer and Dimer Species in Toluene

	TIPS-Tc	TIPS-BT1
Φ_{em}^a	0.74 ± 0.08^b	0.72 ± 0.09^b
$\tau_{\text{obs}}/\text{ns}$	12.5	24.3 ^c
$k_r \times \text{s}$	$(5.9 \pm 0.7) \times 10^7$	$(3.0 \pm 0.4) \times 10^7$
$k_{\text{nr}} \times \text{s}$	$(2.1 \pm 0.2) \times 10^7$	$(1.2 \pm 0.2) \times 10^7$

^aTIPS-Tc and TIPS-BT1 measured relative to coumarin 540A (coumarin 153) in methanol ($\Phi_{\text{em}} = 0.45$). ^bError analysis based on four independent measurements. ^cBased on two independent measurements.

Beginning with the monomeric species, it is seen that TIPS-Tc is a bright emitter ($\Phi_{\text{em}} = 0.74$) whose photoluminescence in room-temperature toluene is well-described by a globally fit, single-exponential decay with a lifetime (τ_{obs}) of 12.5 ns. The time-dependent spectral data and their fits to the single-exponential model (described in the SI) are shown in Figure S2. The basis spectrum from the model agrees with the spectrum observed in steady-state measurements (Figure 3) and reflects $S_1 \rightarrow S_0$ photoluminescence in this molecule. From the observed emission lifetime and quantum yield, radiative (k_r) and nonradiative (k_{nr}) rate constants are determined according to the expression $\Phi_{\text{em}} = k_r/k_{\text{obs}} = k_r/(k_r + k_{\text{nr}}) = k_r \times \tau_{\text{obs}}$. The value of k_r in TIPS-Tc ($5.9 \times 10^7 \text{ s}^{-1}$) is slightly more than double that observed in Tc ($2.4 \times 10^7 \text{ s}^{-1}$), while k_{nr} is smaller by an order of magnitude ($1.9 \times 10^8 \text{ s}^{-1}$ in Tc versus $2.1 \times 10^7 \text{ s}^{-1}$ in TIPS-Tc). This decrease in k_{nr} relative to the parent acene is understood in the context of singlet-to-triplet intersystem crossing (ISC) events involving the S_1 and T_2

states. That process is thought to have a small yield (<6%) in TIPS-Tc,⁵¹ as compared to a substantial (62%, or ~10 times greater) yield in Tc where the states are energetically aligned.⁵²

Turning to the dimer system TIPS-BT1, we first note that $\Phi_{\text{em}} = 0.72 \pm 0.09$ is nearly the same as monomeric TIPS-Tc at 0.74 ± 0.08 (error determined from four independent measurements for each molecule). One might initially intuit that such an observation argues against formation of the optically dark ${}^1\text{TT}$ state (the initial step of SF: $S_1 \rightarrow {}^1\text{TT}$). However, in dimers that are thermo-neutral or endergonic for SF, this is not necessarily the case when the back-reaction ${}^1\text{TT} \rightarrow S_1$ is fast compared to other ${}^1\text{TT}$ loss pathways. In these situations, fluorescence is not ultimately removed from the system, but rather delayed, resulting in the observation of biexponential fluorescence decay kinetics. This is in fact what we saw for BT1 relative to single-exponential decaying Tc and another monomeric model called Tc-e that contains a norbornyl moiety attached to the acene.²¹

To look for delayed fluorescence, time-resolved photoluminescence data were collected for TIPS-BT1 in room-temperature toluene. Quite surprisingly, only single exponential decay kinetics with a time constant of 24.3 ns (Table 1) are observed at all emission wavelengths (see time-dependent spectral data and fits to the single-exponential model in Figure S2). The fitted spectrum from this global model is also shown in Figure S3, and as was seen for the monomer model TIPS-Tc, it agrees with the steady-state measurements (Figure 3). Radiative (k_r) and nonradiative (k_{nr}) rate constants were obtained for TIPS-BT1 in toluene and we will return to a discussion of their values relative to TIPS-Tc (Table 1) after consideration of transient absorption data. For now we simply reiterate that the single exponential decay of S_1 photoluminescence does not support the observation of SF inasmuch as it argues against delayed fluorescence that is tied to ${}^1\text{TT} \rightarrow S_1$ fusion.

Transient Absorption in Toluene. Although the observation was unexpected, there are possibilities for obtaining single exponential S_1 photoluminescence decay kinetics under two scenarios where SF is still operative. The first (i) would be one where ${}^1\text{TT} \rightarrow S_1$ fusion is slow—for example if SF is highly exergonic—and where ${}^1\text{TT}$, once it is formed, is only

nonradiatively removed and serving to repopulate the ground state. In this scenario, the formation of ${}^1\text{TT}$ only serves as a loss pathway in k_{nr} for the S_1 state of the dimer. The second (ii) would be one where an $S_1 \rightleftharpoons {}^1\text{TT}$ equilibrium is established on an ultrafast time scale; i.e., significantly faster than the temporal resolution of our photoluminescence measurement (~ 1 ns). To consider either of these possibilities, we have employed transient absorption measurements.

Transient spectra obtained for the monomer model TIPS-Tc after ultrafast photoexcitation at ~ 530 nm are shown in Figure 4 (top left). These data are consistent with what is reported for

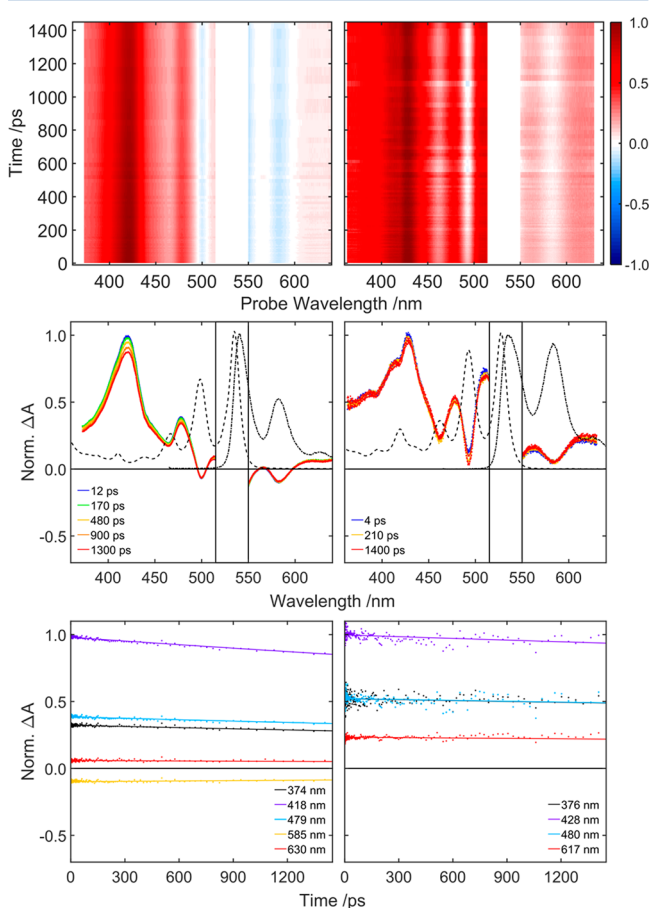


Figure 4. Time-dependent transient absorption surfaces (top), spectra (middle), and kinetics (bottom) for TIPS-Tc (left) and TIPS-BT1 (right) in room temperature toluene. Spectra (middle panels) and kinetics (bottom panels) are extracted from the raw data as points. The lines within the spectra (middle panels) and within the kinetics (bottom panels) are determined from the global fits to the data. Pump scatter has been removed from the TA data.

this molecule in chloroform.⁵¹ The distinct lack of spectral evolution is highly suggestive that the Franck–Condon state is the only one observed during the time delay window of this measurement. In agreement with the PL measurements, this state is the S_1 . In support of this assignment, the transient spectral data are cleanly modeled with a single exponential decay of ~ 10 ns that is independent of wavelength (i.e., a decay that is consistent with the measured fluorescence lifetime). Spectral data at a number of pump/probe delay times are shown in Figure 4 (left middle) along with the obtained fits to the global exponential decay model (a line running through the points for each delay time). The assignment of features is

facilitated by consideration of the static absorption and emission spectra that are shown directly above the data. In general, what is seen is a broad visible transient absorption that is modified (in an attenuating fashion) by the bleach of the $S_1 \leftarrow S_0$ vibronic progression as well as by features attributed to $S_1 \rightarrow S_0$ stimulated emission, in particular the 0–1 emission feature at ~ 580 nm. Given the limited ground-state absorption of TIPS-Tc in the region from ~ 350 nm to ~ 425 nm, the strong transient absorption observed at ~ 425 nm is a distinct and useful indicator of $S_1 \rightarrow S_n$ absorbance, similar to what was observed in another alkynyltetracene dimer.²³

Transient spectra obtained for the TIPS-BT1 dimer are comparable to those of TIPS-Tc, showing a strong ESA at ~ 420 nm, negative features corresponding to bleach of the $S_0 \rightarrow S_1$ vibronic progression, and a negative feature at ~ 580 nm corresponding to stimulated emission of the 0–1 band. Again there is no evidence for spectral evolution at early times (Figure 4 top right) and over the time window of the measurement (1.5 ns) there is little observed decay of features, consistent with an observation of a species whose lifetime is 24 ns. Spectra and kinetic traces shown (middle right and bottom right) have been globally modeled with a 23 ns decay. To further confirm this simple decay and its time scale, a different TA measurement was undertaken capable of measuring longer pump/probe times with an electronic delay rather than a translation stage. Data shown in Figure 5 that range from 0 to 380 ns are spectrally

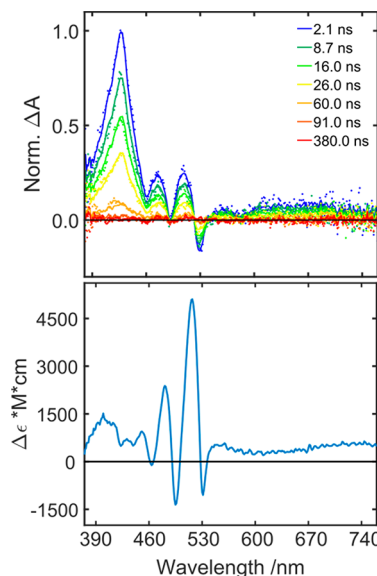


Figure 5. Top: Normalized TA spectra (points) of TIPS-BT1 in toluene following 530 nm excitation over the first 380 ns with slices from the global fit (lines) at the indicated times. Bottom: Sensitized transient spectrum of T_1 for TIPS-BT1 in toluene with accompanying ground-state bleach features (that is, this spectrum includes contributions from ground-state bleach, as expected for a T_1 state formed through SF or ISC).

consistent with the earlier time measurement of Figure 4 (0 to 1.4 ns) and are globally modeled with a single exponential decay of 23.4 ns (see fit spectra in Figure 5). Clearly the transient features that are being observed on a 1 ps time scale are the same as those observed with the longer delay, including the contribution from stimulated emission at ~ 580 nm and including the bright ESA at ~ 420 nm. This latter feature bears a strong similarity to what is seen in the S_1 state of the monomer

(Figure 4 middle left). The decay timescale coincidence and the stimulated emission feature tells us that these TA spectra are observing the same state or manifold of states (vide infra) being interrogated with the time-resolved photoluminescence measurements of Figure S2. These data as a whole argue strongly against the first of the SF-operative scenarios (i) discussed at the beginning of this section. Namely, there is no evidence that the observed state—one that is active toward photoluminescence—has a nonradiative decay channel forming the ${}^1\text{TT}$. Rather, all that we observe in these TA measurements is ground-state recovery with the same rate constant also determined via photoluminescence.

Further support of this conclusion can be found by consideration of a triplet sensitization experiment, the idea being that a hypothetical ${}^1\text{TT}$ or triplet pair in a dimer of weakly coupled chromophores, as we might expect in TIPS-BT1, should bear significant similarity to T_1 , as has been seen in other dimer systems.^{18,19,26} Using photoexcited anthracene as a triplet sensitizer (see a description of the methodology in the SI), the difference spectrum shown in Figure 5 (bottom) was obtained. From the mismatch in spectral features between the sensitized spectrum and the long-time data we can conclude that the ns data shown in Figure 5 (top) argue against ${}^1\text{TT}$ formation. Additionally, there is no evidence outside of the noise of the data for ISC leading to T_1 on its own, giving an upper limit of 5% for T_1 yield, similar to the value reported elsewhere in the TIPS-Tc monomer of 5%.⁵¹

In order to consider the second of the SF-operative scenarios (ii) mentioned above, attention has been focused on earlier times in the TA measurements. First it is reiterated that from the full spectral data shown in Figure 4 (top right), there is no evidence for spectral evolution at early times that would be expected for equilibration of the S_1 with ${}^1\text{TT}$. By carefully examining single wavelength regions, it is nonetheless possible to observe some dynamics. As shown in Figure S5 (left) collected at $\lambda_{\text{probe}} = 429$ nm, a decay can be seen with a time constant of ~ 850 fs that is absent in the monomer model. While SF dynamics on such fast time scales have been reported in other dimer systems, those were cases where energetics and/or coupling were favorable.^{19,23,25–27} Reiterating from the Introduction, static electronic coupling for SF remains zero in TIPS-BT1, just as it was in BT1 where the formation of ${}^1\text{TT}$ takes 70 ns. Given the 5 orders of magnitude difference between 70 ns and the 850 fs, it is highly unlikely that formation of an $\text{S}_1 \rightleftharpoons {}^1\text{TT}$ equilibrium is being observed for TIPS-BT1 on this ultrafast time scale. We instead believe these dynamics are derived from thermalization within the S_1 manifold, discussed below in the context of the emission of TIPS-BT1.

Photophysical Implications for TIPS-BT1 in Toluene. As noted earlier and highlighted in Table 1, the emissive quantum yields (Φ_{em}) are nearly identical for monomeric TIPS-Tc versus dimeric TIPS-BT1 despite the fact that the observed S_1 lifetime across these two species is approximately doubled from 12.5 ns (TIPS-Tc) to 24.3 ns (TIPS-BT1). This becomes possible because k_{r} is nearly halved from 5.9×10^7 in TIPS-Tc to 3.1×10^7 in TIPS-BT1. We find this interesting in reference to the quantitative absorption data (in chloroform) presented earlier where it was shown that the molar extinction effectively tracks the number of chromophores in the molecule. From this perspective alone, one might initially expect that k_{r} for the dimer—as measured using emission following single photoexcitation events per molecule—would be comparable to the

monomer. We can rationalize the k_{r} halving for the dimer by invoking a thermal equilibrium between the emissive state (what we have referred to as S_1) and an energetically lower (but proximal) state that is radiatively dark as can occur in polyenes.⁵³ In our system this is reasonable under circumstances where the emissive and dark states are excitonic in nature and electronically characterized as constructive and destructive (respectively) superpositions of short-axis excitations of the two chromophores of the dimer. Energetic proximity between these states—necessary for the equilibrium that enables room temperature photoluminescence observation from the higher-energy bright state—is entirely reasonable if the chromophores are weakly coupled (as expected from the ratio of 0–0 and 0–1 features in the UV–vis of Figure 3⁴⁷). State proximity is supported by previous time-dependent DFT studies concerning the related dimer BT1. There we observed dark (lower) and bright (higher) vertical states with an energetic separation of 34 meV,¹² that is, reasonably close to kT (25.7 meV) at 298 K. A final point to stress is that these results suggest that the emissive state in TIPS-BT1 in toluene (we will continue to call it S_1) is best characterized as being delocalized over both chromophores. Notably, the TD-DFT studies mentioned above found a lowest energy singlet excited state for BT1 where excitation and nuclear reorganization was localized to one of the two chromophores. These current toluene results argue against such an assignment for TIPS-BT1. We will come back to this point during our exploration of photophysics in the polar environment benzonitrile.

Part 3. Variation in Excited-State Dynamics as Solvent Polarity Is Increased. Photophysics in Benzonitrile. As was noted earlier (see, for example Figure 3), both the monomeric TIPS-Tc and the dimer TIPS-BT1 exhibit a slight bathochromic shift in the absorption onset when the solvent environment is changed from nonpolar toluene to the polar benzonitrile, thus suggestive of so-called “hidden” CT character in the S_1 state.⁴⁹ Notably, however, the band shape similarities between the nonpolar environment and the benzonitrile environment (Figure 3) tell us there is no evidence for photoexcitation of an interchromophore CT state in the dimer TIPS-BT1. In this section, we begin by emphasizing significant qualitative differences in the emission spectrum of TIPS-BT1 versus TIPS-Tc in benzonitrile (Figure 3; bottom left and right) particularly when factoring similarities in their respective absorption profiles. Whereas monomeric TIPS-Tc exhibits strong mirror symmetry between emission and absorption profiles (a property that is consistent in all the solvent environments, not just benzonitrile), the dimer TIPS-BT1 does not and its emission is significantly broadened resulting in a reduction of definition in the vibronic peaks. There are clearly dynamics being captured here that are absent for the monomer and for the dimer explored in the less polar solvents.

Photophysical properties for TIPS-BT1 and TIPS-Tc in room-temperature benzonitrile were measured and are listed in Table 2. In this environment, the monomer TIPS-Tc is a bright emitter with an emissive quantum yield $\Phi_{\text{em}} = 0.90$ that is slightly larger than what is observed in toluene ($\Phi_{\text{em}} = 0.74$; Table 1). The molecule exhibits a time-dependent photoluminescence decay that is cleanly modeled with a single exponential with a time constant (τ_{obs}) of 13.4 ns. Transient absorption data and their fit to a single exponential decay model shown in Figure S6 are consistent with an assignment of S_1 loss to the ground state with this time constant. The quantum yield increase from the monomer in benzonitrile

Table 2. Photophysical Properties Measured for TIPS-Tc and TIPS-BT1 Emission in 293 K Benzonitrile

	TIPS-Tc	TIPS-BT1
$\Phi_{\text{em}}^{\text{a}}$	0.90 ± 0.02	0.52 ± 0.04
lifetime(ns)	$13.4 (\tau_{\text{obs}})$	$12.6 (\tau_{\text{loc}}), 68.2 (\tau_{\text{dim}})$
$k_r \times s$	$(6.7 \pm 0.2) \times 10^7$	not determined
$k_{\text{nr}} \times s$	$(0.76 \pm 0.02) \times 10^7$	not determined

^aMeasured relative to coumarin 480 in methanol;⁵⁴ TIPS-Tc and TIPS-BT1 measured relative to coumarin 540A (coumarin 153) in methanol.⁵⁰

relative to the monomer in toluene is driven by a more than 2-fold decrease in k_{nr} although the origins of this effect (intramolecular versus solvent, or both) are difficult to assign at the moment.

More interesting from our perspective is the substantial drop in emission quantum yield for the dimer versus monomer, from $\Phi_{\text{em}} = 0.90$ (TIPS-Tc) to $\Phi_{\text{em}} = 0.52$ (TIPS-BT1), both in benzonitrile. The decrease in TIPS-BT1 photoluminescence suggests the enhancement of existing nonradiative loss pathways, or the introduction of new ones. Time-dependent emission spectra for TIPS-BT1 in benzonitrile are shown in Figure 6 (top). Of importance is the emergence of a fast

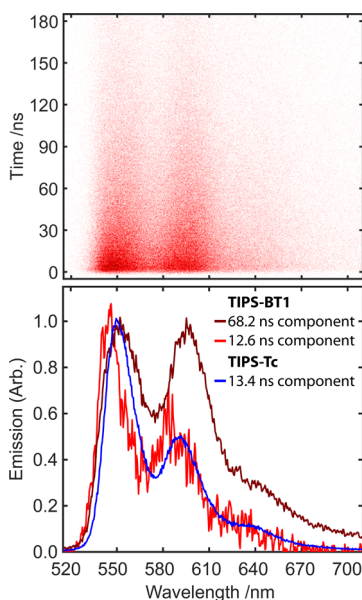


Figure 6. (Top) Normalized photoluminescence spectral decay for TIPS-BT1 in room-temperature benzonitrile after excitation at 493 nm. (Bottom) Normalized basis spectra retrieved from global fits of time-dependent spectral data, with the sole component (lifetime of 13.4 ns) for TIPS-Tc shown in blue (also from benzonitrile solution; see data/fit in Figure S7) and the two decay-associated spectra for TIPS-BT1 shown in light red (component with lifetime of 12.6 ns) and dark red (component with lifetime of 68.2 ns). The spectra shown for TIPS-BT1 have been smoothed using a Savitzky–Golay filter (span of 5 points) for clarity. All analyses used raw (unsmoothed) spectra.

component to the data with slightly blue-shifted spectral properties that is most clearly seen in the first ~ 10 ns. Global analysis of the data reveals two distinct emissive lifetimes of 12.6 and 68.2 ns, with the associated spectral characteristics that are shown in Figure 6 (bottom). These spectra have been normalized, although their true amplitude ratio is very close to what is shown (0.98/1 at the peak for the early/late

components, respectively). Interestingly, the spectrum of the early decay component (light red trace peaked at 545 nm) closely resembles that of the monomer TIPS-Tc whose spectrum is also shown (blue trace). The 0–0 to 0–1 peak ratio in this component indicates an absence of the H-aggregate coupling⁴⁷ of the chromophore pair that was seen for the S_1 state of TIPS-BT1 in toluene (vide supra). It is also striking that the fast emission component in the TIPS-BT1 benzonitrile data decays with a time constant (12.6 ns) that is very similar to the monomer TIPS-Tc decay (13.4 ns). These spectral and temporal data suggest to us that in the solvent benzonitrile, we are observing an arm-localized S_1 excited state for the earlier time component. This is presumably the same type of excited state that we had identified in TD-DFT studies of BT1 where it was referred to as $S_{1\text{-loc}}$ (named for the localization of the excitation).¹² From the average of the peak absorption (Figure 3) and peak emission (Figure 6; light red), $S_{1\text{-loc}}$ for TIPS-BT1 in benzonitrile has an energy of 2.30 eV (Table 3).

The second spectral component from the time-resolved emission data is red-shifted (by 30 meV) relative to the $S_{1\text{-loc}}$ emission peak and has a strikingly different ratio of 0–0 to 0–1 features, indicating coupling between the chromophores⁴⁷ just as was seen for the toluene data. This state is henceforth called $S_{1\text{-dim}}$ with the name referring to our assignment that it is from a dimer-delocalized S_1 excited state. It is worth noting that in our previous TD-DFT study of BT1 (with a toluene-parametrized continuum model), we identified a geometry-optimized excited state that was referred to as $S_{1\text{-deloc}}$. However, that state was found to be higher in energy than $S_{1\text{-loc}}$ by 140 meV, and we believed (though computational costs precluded diagonalization of the Hessian) that it was likely to be a transition state between the two different arm-localized excited states ($S_{1\text{-loc}}$ on either side of the BT1 dimer). At this point, it is not clear whether the DFT-identified $S_{1\text{-deloc}}$ is in fact a stationary state in BT1 comparable to the $S_{1\text{-dim}}$ state we are observing here in TIPS-BT1 in benzonitrile, or whether $S_{1\text{-dim}}$ is a different dimer-delocalized entity that we previously missed in our computational explorations.

Temperature-Dependent Steady-State Emission. Given the dual-emission quality of the TIPS-BT1 emission data in benzonitrile, we turned to temperature-dependent experiments to explore the relationship between the observed states. Steady-state photoluminescence measurements were carried out on TIPS-Tc and TIPS-BT1 in toluene and benzonitrile at temperatures ranging between 275 and 315 K, and the results are shown in Figure 7. The relative emission values (Φ_{rel}) were obtained by computing the emission quantum yield at each temperature relative to coumarin 540A in room temperature methanol⁵⁰ and then dividing the result by the measured Φ_{em} at 293 K (20 °C). Linear fits are given as solid and dashed lines to guide the eye. The emission spectra of TIPS-BT1 at each temperature are shown in Figure S8, where each individual spectrum has been scaled to reflect the measured Φ_{em} at the indicated temperature relative to Φ_{em} at 293 K in the corresponding solvent (monomer spectra are also shown in Figure S8).

In the monomer TIPS-Tc, there is very little change observed for Φ_{rel} in either solvent with increasing temperature. In toluene, deviation from the reference (293 K) emission signal is small (~4%) and shows an overall systematic decrease with temperature. In benzonitrile, changes are again small (~4%) and again suggest a systematic decrease, albeit even less pronounced than in toluene. The behavior of the dimer TIPS-

Table 3. Absorption and Emission Energies in Room-Temperature Toluene and Benzonitrile

state	energy in toluene/eV	energy in benzonitrile/eV
$S_1 \leftarrow S_0$ (absorption) ^a	2.35	2.33
$S_{1\text{-dim}}$ (emission) ^a	2.32	2.25
$S_{1\text{-dim}}$ ^b	2.33	2.29
$S_{1\text{-loc}}$ (emission) ^a	N.A.	2.28
$S_{1\text{-loc}}$ ^b	N.A.	2.30

^aEnergies taken from the center of 0–0 absorption or emission features as noted in parentheses. ^bEstimated from the average of the corresponding 0–0 absorption and emission features.

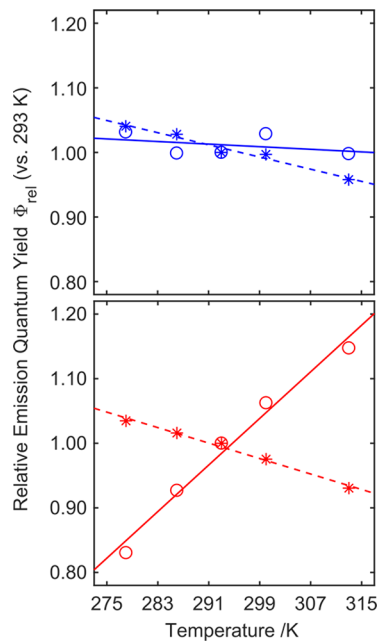


Figure 7. Temperature dependence of Φ_{em} for TIPS-Tc (blue, top) and TIPS-BT1 (red, bottom) in toluene (asterisks, fits as dashed lines) and benzonitrile (open circles, fits as solid lines) between 275 and 315 K. Values of Φ_{rel} for each solvent were obtained by scaling Φ_{em} at each temperature to its value at 293 K. Corresponding spectra are available in Figure S8.

BT1 in toluene is similar to that of TIPS-Tc, with a small systematic decrease in Φ_{rel} as the temperature increases (not exceeding ~7% of the initial value). The reason for the slightly increased strength of the observed temperature effect is unclear, although it is possibly due to an increase in the number of vibrational degrees of freedom available to TIPS-BT1 relative to TIPS-Tc. Spectral changes upon heating and cooling are minimal, with a minor increase in the ratio of 0–0 to 0–1 peak heights evident as temperature is increased.

In benzonitrile, TIPS-BT1 exhibits a startling increase in emission quantum yield with temperature that exceeds 15% of the reference (293 K) value at the extremes of the temperature range investigated (see both top and bottom panels of Figure 7). Seeking explanations, we turned to time-dependent photoluminescence data collected as a function of temperature.

Temperature-Dependent Time-Resolved Photoluminescence. Using a cryostat in the spectrometer, time-dependent photoluminescence data sets were collected for TIPS-BT1 at 273, 296, and 323 K in both toluene and benzonitrile. Just as before (Part 2), a single exponentially decaying spectrum is adequate for cleanly modeling—at each temperature—the toluene data, whereas two decaying functions are needed to cleanly model the TIPS-BT1 in benzonitrile data. The resulting

time-resolved photoluminescence (TRPL) basis spectra from these global fits are given in Figure S9. There it can be seen that temperature-dependent spectral changes are quite subtle, and we do not address them further here. The corresponding lifetimes for each temperature and the extracted per-state emission yields are summarized in Table 4. Full TRPL data and spectral slices with corresponding fits are shown in the SI (Figure S10 and S11) for all data sets.

Table 4. Temperature-Dependent Data from TRPL of TIPS-BT1, Including Emissive Lifetimes and Relative Emission of Individual States

component (solvent)	temperature /°C	state lifetime, τ_n /ns	emission fraction, $F_n(T)$	relative emission $\Phi_{\text{rel},n}(T)$
S_1 (toluene)	273	25.3	1	1.05
	296	25.1	1	0.99
	323	26.0	1	0.90
$S_{1\text{-loc}}$ (benzonitrile)	273	13.4	0.13	0.10
	296	12.6	0.10	0.11
	323	13.0	0.08	0.10
$S_{1\text{-dim}}$ (benzonitrile)	273	75.0	0.87	0.70
	296	68.2	0.90	0.91
	323	57.0	0.92	1.15

TIPS-BT1 in toluene exhibits monoexponential photoluminescence decays at all temperatures with no systematic changes in the observed lifetime versus temperature. Findings for TIPS-BT1 in benzonitrile are yet again markedly different from those in toluene. Biexponential global fitting reveals the same two spectral components ($S_{1\text{-loc}}$ and $S_{1\text{-dim}}$) at all temperatures, but their behavior with temperature differs noticeably. The $S_{1\text{-loc}}$ component has no temperature-dependence whereas the $S_{1\text{-dim}}$ component becomes systematically shorter-lived as temperature is increased. The temperature-dependent decrease of the $S_{1\text{-dim}}$ lifetime (τ_{dim}) suggests that the concomitant increase to Φ_{em} (Figure 7) does not stem from a decrease to k_{nr} . Given that $\Phi_{\text{em}} = k_r/(k_r + k_{\text{nr}}) = k_r \times \tau_{\text{obs}}$, a decrease to k_{nr} (for the dimer) is expected to increase τ_{dim} and in turn increase Φ_{em} . There is a possibility that an increase in k_r with temperature is the origin of the observation; however, we find that scenario to be unlikely. While relatively rare, there are known systems where k_r varies with temperature, but these are typically chromophores exhibiting significant conformational flexibility, such as in twisted intramolecular charge transfer states, where emission from otherwise unstable molecular configurations becomes thermally activated.⁵⁵ Such behavior should not be expected for TIPS-BT1 (in $S_{1\text{-loc}}$ or $S_{1\text{-dim}}$) with its rigid norbornyl bridge between chromophoric subunits.

In order to gain insight, we have calculated from the data two quantities referred to as $F_n(T)$ and $\Phi_{\text{rel},n}(T)$ (listed in Table 4 and derived in the SI.). The first is the fraction (at temperature

T) of emitted photons from either of the n states $S_{1\text{-loc}}$ or $S_{1\text{-dim}}$. For example at 273 K (see Table 4), 13% of the emitted photons are from $S_{1\text{-loc}}$ and 87% are from $S_{1\text{-dim}}$. The second quantity $\Phi_{\text{rel},n}(T)$ describes the number of photons emitted by state n at temperature T compared to the total number of photons emitted by the molecule at 293 K. Use of $\Phi_{\text{rel},n}(T)$ permits quantification of individual contributions from $S_{1\text{-loc}}$ and $S_{1\text{-dim}}$ toward the temperature-dependence seen in Figure 7 (top). This metric is helpful since neither the per-state emission quantum yield nor the per-state fraction of the overall excited population is known for these states. The findings from this analysis rule out thermally driven population transfer between $S_{1\text{-loc}}$ and $S_{1\text{-dim}}$: the quantity of emission from $S_{1\text{-loc}}$ ($\Phi_{\text{rel},\text{loc}}(T)$) remains small and approximately constant as temperature is changed (0.10, 0.11, and 0.10 at 273, 296, and 323 K, respectively), while emission from $S_{1\text{-dim}}$ ($\Phi_{\text{rel},\text{dim}}(T)$) changes markedly (0.70, 0.91, and 1.15 at 273, 296, and 323 K, respectively). In toluene, the per-state emission quantum yield is trivially identical to the Φ_{rel} values plotted in Figure 7 (top).

The most probable explanation for the temperature-dependent emission of TIPS-BT1 in benzonitrile is that a lower-energy nonemissive (dark) state exists in equilibrium with the emissive $S_{1\text{-dim}}$. That is, under the constraint that the total population of these states is conserved (dark state plus $S_{1\text{-dim}}$), the emission that is reflected in $\Phi_{\text{rel},\text{dim}}$ (and eventually Φ_{rel}) may be increased by redistributing excited-state populations to favor the emissive state. Finally, it is reiterated that this equilibrium exists concurrently with, and isolated from, the faster monoexponential decay of $S_{1\text{-loc}}$.

Transient Absorption Dynamics in Room-Temperature Benzonitrile. In this section of the paper, the tool of transient absorption spectroscopy is revisited to better understand the nature of the nonemissive state implicated in the temperature-dependent emission studies discussed above, and to explore how the equilibrium between it and $S_{1\text{-dim}}$ is established. As was done previously for measurements in toluene, findings are first reported for the monomer TIPS-Tc in benzonitrile. Figure S6 shows transient absorption spectra collected at various times within the first 1.4 ns after ultrafast photoexcitation at 530 nm. These data bear strong resemblance to the TIPS-Tc in toluene data shown in Figure 4, with equivalent features that are again cleanly modeled using a single exponential decay. Within experimental error (given the 1.4 ns length of the femtosecond TA experiment), the time constant found here (~ 10 ns) matches the time constant measured via TRPL ($\tau_{\text{obs}} = 13.4$ ns, *vide supra*) wherein we monitored the decay of the S_1 state of the monomer to the ground state by radiative (k_r) and nonradiative (k_{nr}) pathways.

By contrast, TA data for the dimer TIPS-BT1 differ markedly as the polarity of the solvent is changed prompting us to show side-by-side in Figure 8 the benzonitrile data (right) next to the toluene data (left) that was previously reported in Figure 4. Before discussing the differences, it is first noted that at early times, for example at $\Delta t = 4$ ps, the TA spectral data (middle panels) for TIPS-BT1 in the two solvents are very similar. This indicates that $S_{1\text{-dim}}$ is rapidly formed in benzonitrile just as it was in toluene. Ultrafast kinetic traces shown in Figure S5 (right) again indicate a subpicosecond component for the dimer in benzonitrile that is absent from the monomer (where only a coherence spike is observed). As was the case for the toluene data, this 675 fs component is attributed to thermalization within the $S_{1\text{-dim}}$ manifold where a slightly lower-energy dark state is populated on a rapid time scale after

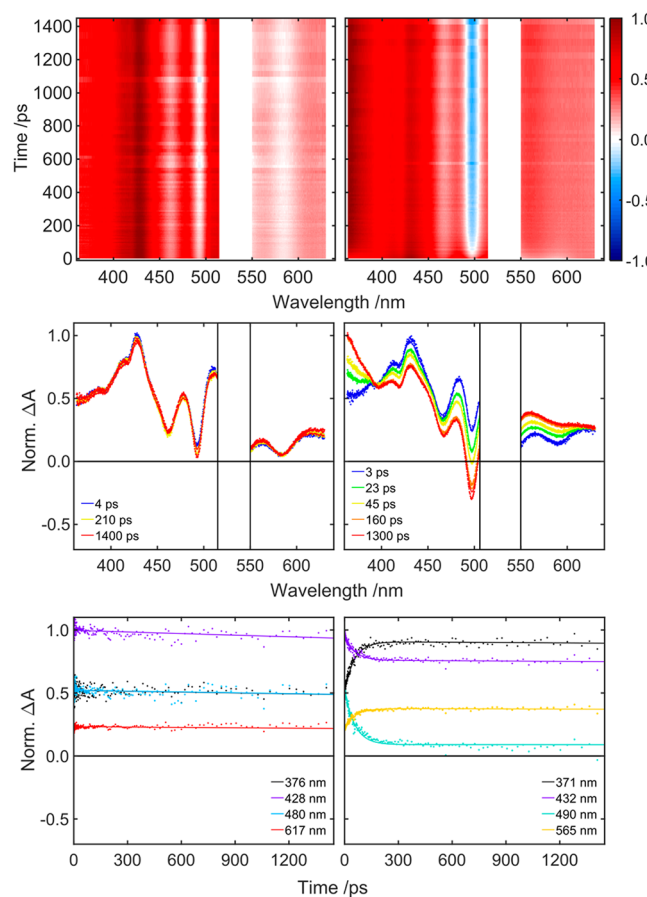


Figure 8. TIPS-BT1 fsTA surfaces (top), spectra (middle), and kinetics (bottom) in toluene (left) and benzonitrile (right). Spectra and kinetics are extracted from the data (points) and from the global fit (lines). Pump scatter has been removed for clarity.

photoexcitation into a bright Franck–Condon state. On the ultrafast time scale, we do not observe separate dynamics that might be attributed to relaxation to the emissive $S_{1\text{-loc}}$ state observed in the TRPL studies discussed above. This indicates that the photoexcitation pulse simultaneously accesses the localized and delocalized S_1 manifolds (i.e., their formation is near-concurrent rather than sequential) and that relaxation dynamics following Franck–Condon excitation into the $S_{1\text{-loc}}$ surface are subtle, similar to the monomer, in which no dynamics are observed.

Turning to times beyond the $\Delta t = 4$ ps discussed above, the TA spectral data for TIPS-BT1 in benzonitrile show a clear evolution between two states with the maintenance of a TA isosbestic point at 393 nm. This evolution occurs with a time scale of 50 ps as seen in the kinetic slices (Figure 8 (bottom right)) with accompanying fits to a two-exponential model (50 ps and a much longer ~ 10 ns component). Within the spectral data, a new ESA feature emerges with its peak in the UV (beginning near 390 nm and continuing outside of the 360 nm probe limit of the experiment) and a second ESA appears with onset near 550 nm. There is a concurrent loss of ESA throughout the region between 400 and 550 nm and a loss of stimulated emission to the red of 550 nm. These losses tie to features that are also present in the toluene TIPS-BT1 data (i.e., features attributed to $S_{1\text{-dim}}$). It is also clear from these data that the interconversion between states is not complete. Whereas the dynamics cease by ~ 200 ps (see the TA spectral

comparison between 160 and 1300 ps), features remain at long times (e.g., 1300 ps)—for example the strong two-humped TA absorption between 400 and 440 nm—that are present at the onset of the dynamics. This is of course consistent with the establishment of an equilibrium between $S_{1\text{-dim}}$ and a dark state (that was implied by the temperature-dependent emission data), and this notion is further borne out by transient absorption measurements on the nanosecond time scale (discussed at the end of this section).

Given the nature of TIPS-BT1, there are, in our estimation, two potential assignments that could be made for the dark state that equilibrates with $S_{1\text{-dim}}$ in 50 ps. The first is the ^1TT that is integral to SF while the second is an intradimer CT state (presumably ^1CT). Significant involvement of ^1TT strikes us as unlikely. As discussed in the **Introduction**, symmetry considerations germane to BT1 still argue against substantial electronic interaction between $S_{1\text{-dim}}$ and ^1TT , and we recall our earlier conclusion that there is no evidence for ^1TT formation for TIPS-BT1 in toluene. The question then emerges as to whether the polar environment of benzonitrile could meaningfully alter the driving force of this reaction so as to make it prompt even without substantial electronic coupling between reactant and product states. To argue against this, we note the energetic similarity of $S_{1\text{-dim}}$ in benzonitrile (2.29 eV; **Table 3**) versus toluene (2.33 eV; **Table 3**) and suggest that in light of this, it is difficult to justify why ^1TT would be specifically and significantly stabilized in the polar environment above and beyond $S_{1\text{-dim}}$.

Turning to the second dark-state possibility (^1CT), we first consider electrochemical properties of TIPS-BT1 (and TIPS-Tc) in benzonitrile in order to quantify redox potentials and to estimate CT energetics. Redox potentials were measured using cyclic voltammetry in benzonitrile solutions with supporting electrolyte and are listed in **Table S4**. As can be seen through comparison between TIPS-Tc and TIPS-BT1 data, the norbornyl bridge of the dimer has only a minor impact—of order 10 mV—on the potential needed for generation of the acene radical anion. This suggests that monomer models of these dimer systems can serve as reasonable surrogates for estimation of CT-state energetics or for spectroelectrochemical studies (vide infra). To arrive at energies, the framework of Weller is applied wherein the $\Delta E_{1/2}$ value (one-electron oxidation potential minus the one-electron reduction potential) is modified (lowered) by a Coulomb attraction term that factors the expected distance of charge separation for a CT state in the dimer as well as the dielectric constant of the solvent (25.9 for benzonitrile).^{56,57} We assume opposite point charges at a separation distance of 10.5 Å taken from the approximate center-to-center distance of the acene arms in TIPS-BT1 (again measured based on a DFT-optimized ground-state geometry with the same method used for BT1¹²). These simple Coulombic calculations applied to TIPS-BT1 suggest a CT-state energy of 2.21 eV, a value that is slightly lower than our estimate for the $S_{1\text{-dim}}$ energy from the emission studies (2.29 eV; **Table 3**). This supports the idea that in benzonitrile, the ^1CT state can reasonably function as the dark state in equilibrium with $S_{1\text{-dim}}$.

This idea is further supported using spectroelectrochemical experiments. Given that a CT state in the dimer should consist of an oxidized and a reduced chromophore arm, we sought to approximate these species through spectroelectrochemistry of the monomer. This is further justified by the previously mentioned similarity between monomer/dimer redox behavior.

Results in benzonitrile are shown in **Figure 9**, in which both the oxidative and reductive components have been normalized to

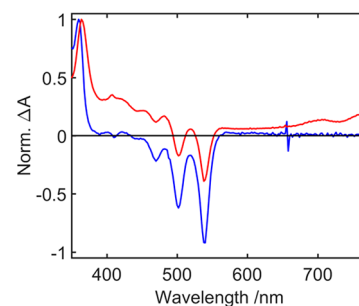


Figure 9. Absorption difference spectra (normalized) of TIPS-Tc in benzonitrile following oxidative (blue) and reductive (red) bulk electrolysis in an optically transparent electrochemical cell. The small feature at 650 nm (oxidative component) is an instrument-related artifact.

their largest absorptive feature. Beyond the loss of $S_1 \leftarrow S_0$ vibronic progression (~450 nm – 550 nm), the most prominent feature is an absorption peak in the UV that is present (albeit slightly shifted) following both oxidation (blue) and reduction (red). For the reduction difference spectrum, absorption continues into the visible (until 494 nm) and again broadly in the red with an onset near 560 nm that continues to lower energy. Although these spectra are qualitative (i.e., no effort was made to quantify the relative magnitude of the absorptive and reductive components), their features are consistent with ones emerging in the first 50 ps of excited-state evolution of TIPS-BT1 in benzonitrile (**Figure 8** (right)). Most importantly, both the bright UV feature and the broad visible feature at wavelengths greater than ~550 nm that emerge in the TA data match absorptions attributed to redox events.

Nanosecond Transient Absorption Dynamics and Triplet Sensitization. As a final point of discussion, we address experiments designed to explore the fate of the $S_{1\text{-dim}}/{}^1\text{CT}$ state equilibrium in benzonitrile. Global fitting of a transient absorption data set collected with nanosecond time resolution (**Figure 10**) exposes two species that decay with lifetimes of 13.7 and 67.4 ns, values that match those from TRPL (12.6 and 68.2 ns).

The decay-associated TA spectrum for the fast (13.7 ns) component shown in **Figure 11** (bottom; lighter red trace) has a strong correspondence with transient spectra taken for the

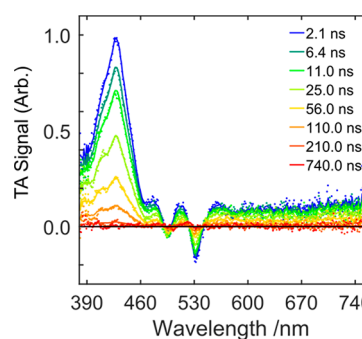


Figure 10. TA spectra of TIPS-BT1 in room temperature benzonitrile following 530 nm excitation over the first 740 ns with the global fit (lines) at the indicated times.

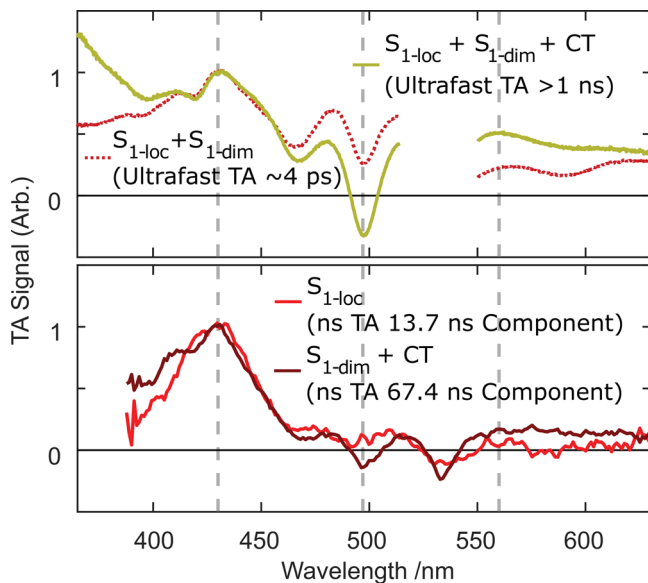


Figure 11. Spectra from global fits of TIPS-BT1 in benzonitrile (normalized to the ~430 nm ESA). Top: Ultrafast TA spectra extracted from the beginning (red dotted line, contains contributions from $S_{1\text{-loc}}$ and $S_{1\text{-dim}}$) and end (yellow solid line, contains contributions from $S_{1\text{-loc}}$, $S_{1\text{-dim}}$, and CT) of the global fit. Bottom: ns TA basis spectra for the short-lifetime component (red, pure $S_{1\text{-loc}}$) and long-lifetime component (dark red, $S_{1\text{-dim}} + CT$) from the ns TA experiment. Vertical dashed lines show alignment of 433 nm ESA, 498 nm GSB, and 560 nm ESA between species (as applicable).

monomer model TIPS-Tc (Figure S6), thus agreeing with the TRPL assignment of this lifetime to $S_{1\text{-loc}}$. The decay-associated spectrum for the longer (67.4 ns) component (Figure 11 (bottom; darker red trace)) shows a superposition of features consistent with equilibrium between the ^1CT (e.g., the onset of ESA to the blue of 400 nm and to the red of 550 nm) and $S_{1\text{-dim}}$ (e.g., the strong ESA at 433 nm). For completeness, Figure 11 shows a comparison of the 67.4 ns decay-associated spectrum (dark red trace; bottom) with a spectrum (dark yellow trace; top) extracted from the global fit to the ultrafast TA data (Figure 8) at 1400 ps; i.e., well after the 50 ps equilibration between $S_{1\text{-dim}}$ and ^1CT . The two spectra are in agreement, with the caveat that the data from the faster measurement (dark yellow trace; top) contains additional information from $S_{1\text{-loc}}$ population that has not yet decayed away.

That all features in Figure 10 (both positive and negative) decay toward $\Delta A = 0$ supports the earlier finding from TRPL that $S_{1\text{-loc}}$ and $S_{1\text{-dim}}$ (which later equilibrates with the dark ^1CT) do not interconvert. In other words, one state does not feed into the other during the dynamics; namely, there is no evidence for the rise of a feature concurrent with the decay of another. We also emphasize that there is no appreciable evidence in the TA spectral data at long times (e.g., at 740 ns) for production of the lowest energy triplet. Assuming that the $\Delta\epsilon$ spectrum collected using triplet sensitization of TIPS-BT1 would be similar in benzonitrile to that in toluene (Figure 5) we model that the triplet yield in benzonitrile is less than 5% and within the noise of the ns TA measurement. This is interesting in light of observations by Johnson and co-workers of several diphenyl isobenzofuran dimers where the CT manifold mediates appreciable T_1 production via the following pathway: $^1\text{CT} \rightarrow ^3\text{CT} \rightarrow T_1$.¹¹ These results in TIPS-BT1 support the earlier assignment that the $S_{1\text{-dim}}/\text{CT}$ equilibrium is

within the singlet manifold as rapid internal conversion ($^3\text{CT} \rightarrow T_1$) would be expected if ^3CT were involved. Further it suggests that the primary pathway for decay of ^1CT is nonradiative coupling to the ground state as well as the radiative bleeding due to its coupling to the bright $S_{1\text{-dim}}$ state.

III. SUMMARY AND CONCLUSIONS

A number of conclusions can be drawn and we summarize our findings by first discussing results obtained in nonpolar toluene to be followed in subsequent paragraphs by a discussion of findings in the polar medium benzonitrile. In toluene, TIPS-BT1 absorbs into and subsequently emits from a single electronic state that is dimer-delocalized. It is electronically derived from the bright member of an excitonic pair within a weakly coupled H-aggregate of acene chromophores, where the emission transition is short-axis polarized. In TA data (resolved on both femtosecond and nanosecond time scales) only two processes are observed: a minor subpicosecond relaxation and a long-lifetime decay that tracks the time-dependence of the emission spectrum. The subpicosecond feature is unlikely to be derived from SF-related processes given symmetry arguments that impact diabatic coupling between states in the $S_1 \rightarrow ^1\text{TT}$ photoreaction and the fact that in the related BT1 dimer, this process takes 70 ns. The single exponential loss of S_1 and the absence of T_1 features in the TA argues that S_1 decays to the ground state via radiative and nonradiative pathways, the latter of which does not include appreciable intersystem crossing (<5% by the noise in our measurements). Importantly, there is no evidence for delayed fluorescence in TIPS-BT1 that would implicate $^1\text{TT} \rightarrow S_1$. This was initially surprising, given that it is observed for BT1, and reaction energetics may play an important role in this overall observation. The (triisopropylsilyl)acetylene substituents in TIPS-BT1 are observed to significantly stabilize the S_1 state (2.33 eV) compared to the unsubstituted BT1 (2.62 eV²¹). If the ^1TT in TIPS-BT1 is parent-acene localized—i.e., if it is not appreciably stabilized by the (triisopropylsilyl)acetylene substituents—then the photoreaction in this dimer would be significantly endergonic. One experimental estimate of the T_1 energy for TIPS-Tc places it at 1.25 eV,⁵¹ implying that $2 \times T_1$ may lie near ~2.5 eV in the dimer—significantly uphill from S_1 . That property, along with the poor diabatic coupling for the $S_1 \rightarrow ^1\text{TT}$ photoreaction, may limit the importance of the fission pathway in this dimer in nonpolar media.

In the polar benzonitrile environment, there are two notable observations concerning the excited-state dynamics of TIPS-BT1. First, visible excitation appears to partition excited-state population into both dimer-delocalized and dimer-localized $\pi-\pi^*$ states ($S_{1\text{-dim}}$ and $S_{1\text{-loc}}$, respectively). Temperature dependent time-resolved photoluminescence measurements as well as ns-resolved TA measurements suggest that these populations are isolated from one another. The $S_{1\text{-loc}}$ decays to the ground state via radiative and nonradiative pathways in much the same way (and with the same absorptive and emissive spectral characteristics and lifetime) as the monomer model TIPS-Tc. These findings are in our view quite remarkable. They suggest that in the polar benzonitrile environment a significant energetic barrier exists for interconversion between the $S_{1\text{-dim}}$ and $S_{1\text{-loc}}$ states even in a system that while exploring marked acene bond-length changes across these states cannot explore conformational isomers in the traditional sense of large amplitude motions.²² There is precedent for solvent-driven localization versus delocalization in intramolecular CT

dimers,^{58–60} but there, solvent reorganization is understandably important. The fact that we observe effects in benzonitrile but not in toluene may further implicate the “hidden” CT character in acene singlet excited states⁴⁹ for affecting relaxation dynamics of the system as a whole.

The second notable observation for TIPS-BT1 involves the dynamics of the population partitioned into the $S_{1\text{-dim}}$ manifold. In 50 ps, a two-state equilibrium is established, involving $S_{1\text{-dim}}$ and a dark state. It is, we believe, unreasonable to conclude that this second state is the ^1TT and rather conclude, based on spectroelectrochemical evidence and the fact that the dimer is in a highly polar environment, that the dark state is the ^1CT . TA and TRPL measurements suggest the two states decay together with a lifetime (67.8 ns, average of TRPL and ns-resolved TA measurements) that is separate from $S_{1\text{-loc}}$. As in the toluene ns TA data, there is no evidence above the noise for formation of long-lived triplets, suggesting that in benzonitrile the pathway $^1\text{CT} \rightarrow ^3\text{CT} \rightarrow \text{T}_1$ is not important in the decay dynamics.

These TIPS-BT1 results contribute to a growing body of evidence that CT-state energies are mechanistically important in $S_1 \rightarrow ^1\text{TT}$ conversion. When the CT state is too high, its contribution to diabatic coupling between these states is minimized. Along with symmetry and reaction energetics, this contributes to a reaction that is slow for BT1²¹ and not observed for TIPS-BT1 in toluene. Others have observed SF enhancement by changing CT energetics in Pc -dimers.^{18,25,27} Finally, when the CT state is too low, it serves as a trap state as has been seen here for TIPS-BT1 in benzonitrile as well as in diphenylisobenzofuran dimers¹¹ and terylene bis(dicarboximide) dimers.²⁶

As a means of informing future studies, the basic platform of the TIPS-BT1 molecule has promise. As a parent dimer chromophore, it is far more extensible than BT1 due to its improved solubility, stability, and reduced nonradiative loss due to ISC. Motifs for subsequent investigations can explore, in a controlled fashion, the role of energetics as well as electronic coupling for the primary $S_1 \rightarrow ^1\text{TT}$ photoreaction. For example, comparable TIPS-acetylene-substituted symmetric pentacene (Pc) dimers that have now been synthesized in our group should isolate the role of energetics in facilitating otherwise forbidden (by symmetry) SF.³¹ Given the conformational flexibility present in the vast majority of other dimer systems, this is an area that is largely unexplored. Studies of asymmetric TIPS-acetylene-substituted Tc dimers will allow for comparison of predicted SF rates against experiment, testing theories about how diabatic coupling can be controlled using symmetry properties. Finally, asymmetric Pc dimers should give rise to very fast and efficient SF and allow for testing of the limits of efficient SF in the solution phase.

ASSOCIATED CONTENT

Supporting Information

The Supporting Information is available free of charge on the ACS Publications website at DOI: [10.1021/acs.jpca.7b09458](https://doi.org/10.1021/acs.jpca.7b09458).

Experimental and computational methods are provided in the Supporting Information (SI) along with additional data Figures (S1–S11), Tables (S1–S7), discussion of absorption spectral feature assignments, explanation of fitting and sensitization procedures, and derivation of temperature-dependent metrics ([PDF](#))

AUTHOR INFORMATION

Corresponding Author

*E-mail: niels.damrauer@colorado.edu. Tel.: 303-735-1280.

ORCID

Dylan H. Arias: [0000-0003-2358-6967](https://orcid.org/0000-0003-2358-6967)

Justin C. Johnson: [0000-0002-8874-6637](https://orcid.org/0000-0002-8874-6637)

Niels H. Damrauer: [0000-0001-8337-9375](https://orcid.org/0000-0001-8337-9375)

Notes

The authors declare no competing financial interest.

ACKNOWLEDGMENTS

For initial stages of this research, we acknowledge support from the Chemical Sciences, Geosciences, and Biosciences Division, Office of Basic Energy Science, U.S. Department of Energy through grant DE-FG02-07ER15890. For later stages of this research, we acknowledge support from the National Science Foundation through grant CHE-1665375. We thank Orion Pearce, James Utterback, and Professor Gordana Dukovic for help measuring certain nanosecond TA decay dynamics. This work utilized resources at the National Energy Research Scientific Computing Center, which is supported by the Office of Science of the U.S. Department of Energy under Contract No. DE-AC02-05CH11231. D.H.A. and J.C.J. acknowledge support from the U.S. Department of Energy, Office of Basic Energy Sciences, Division of Chemical Sciences, Biosciences, and Geosciences, through Contract No. DE-AC36-08GO28308 with NREL enabling their assistance with fluorescence lifetime and triplet sensitization measurements.

REFERENCES

- (1) Hanna, M. C.; Nozik, A. J. Solar Conversion Efficiency of Photovoltaic and Photoelectrolysis Cells with Carrier Multiplication Absorbers. *J. Appl. Phys.* **2006**, *100*, 074510.
- (2) Beard, M. C.; Luther, J. M.; Semonin, O. E.; Nozik, A. J. Third Generation Photovoltaics Based on Multiple Exciton Generation in Quantum Confined Semiconductors. *Acc. Chem. Res.* **2013**, *46*, 1252–1260.
- (3) Pope, M.; Swenberg, C. E. *Electronic processes in organic crystals and polymers*; 2nd ed.; Oxford University Press: New York, 1999.
- (4) Smith, M. B.; Michl, J. Singlet Fission. *Chem. Rev.* **2010**, *110*, 6891–6936.
- (5) Singh, S.; Jones, W. J.; Siebrand, W.; Stoicheff, B. P.; Schneider, W. G. Laser Generation of Excitons and Fluorescence in Anthracene Crystals. *J. Chem. Phys.* **1965**, *42*, 330–342.
- (6) Swenberg, C. E.; Stacy, W. T. Bimolecular Radiationless Transitions in Crystalline Tetracene. *Chem. Phys. Lett.* **1968**, *2*, 327–328.
- (7) Merrifield, R.; Avakian, P.; Groff, R. P. Fission of Singlet Excitons into Pairs of Triplet Excitons in Tetracene. *Chem. Phys. Lett.* **1969**, *3*, 386–388.
- (8) Smith, M. B.; Michl, J. Recent Advances in Singlet Fission. *Annu. Rev. Phys. Chem.* **2013**, *64*, 361–386.
- (9) Müller, A. M.; Avlasevich, Y.; Mullen, K.; Bardeen, C. J. Evidence for Exciton Fission and Fusion in a Covalently Linked Tetracene Dimer. *Chem. Phys. Lett.* **2006**, *421*, 518–522.
- (10) Müller, A. M.; Avlasevich, Y. S.; Schoeller, W. W.; Müllen, K.; Bardeen, C. J. Exciton Fission and Fusion in Bis(Tetracene) Molecules with Different Covalent Linker Structures. *J. Am. Chem. Soc.* **2007**, *129*, 14240–14250.
- (11) Johnson, J. C.; Akdag, A.; Zamadar, M.; Chen, X.; Schwerin, A. F.; Paci, I.; Smith, M. B.; Havlas, Z.; Miller, J. R.; Ratner, M. A.; et al. Toward Designed Singlet Fission: Solution Photophysics of Two Indirectly Coupled Covalent Dimers of 1,3-Diphenylisobenzofuran. *J. Phys. Chem. B* **2013**, *117*, 4680–4695.

(12) Vallett, P. J.; Snyder, J. L.; Damrauer, N. H. Tunable Electronic Coupling and Driving Force in Structurally Well-Defined Tetracene Dimers for Molecular Singlet Fission: A Computational Exploration Using Density Functional Theory. *J. Phys. Chem. A* **2013**, *117*, 10824–10838.

(13) Bula, R.; Fingerle, M.; Ruff, A.; Speiser, B.; Maichle-Mossmer, C.; Bettinger, H. F. Anti-[2.2](1,4)pentacenophane: a Covalently Coupled Pentacene Dimer. *Angew. Chem., Int. Ed.* **2013**, *52*, 11647–11650.

(14) Akdag, A.; Wahab, A.; Beran, P.; Rulisek, L.; Dron, P. I.; Ludvik, J.; Michl, J. Covalent Dimers of 1,3-Diphenylisobenzofuran for Singlet Fission: Synthesis and Electrochemistry. *J. Org. Chem.* **2015**, *80*, 80–89.

(15) Alguire, E. C.; Subotnik, J. E.; Damrauer, N. H. Exploring Non-Condon Effects in a Covalent Tetracene Dimer: How Important Are Vibrations in Determining the Electronic Coupling for Singlet Fission? *J. Phys. Chem. A* **2015**, *119*, 299–311.

(16) Damrauer, N. H.; Snyder, J. L. Symmetry-Directed Control of Electronic Coupling for Singlet Fission in Covalent Bis-Acene Dimers. *J. Phys. Chem. Lett.* **2015**, *6*, 4456–4462.

(17) Lukman, S.; Musser, A. J.; Chen, K.; Athanasopoulos, S.; Yong, C. K.; Zeng, Z. B.; Ye, Q.; Chi, C. Y.; Hodgkiss, J. M.; Wu, J. S.; et al. Tuneable Singlet Exciton Fission and Triplet-Triplet Annihilation in an Orthogonal Pentacene Dimer. *Adv. Funct. Mater.* **2015**, *25*, 5452–5461.

(18) Zirzlmeier, J.; Lehnher, D.; Coto, P. B.; Chernick, E. T.; Casillas, R.; Basel, B. S.; Thoss, M.; Tykwienski, R. R.; Guldi, D. M. Singlet Fission in Pentacene Dimers. *Proc. Natl. Acad. Sci. U. S. A.* **2015**, *112*, 5325–5330.

(19) Sanders, S. N.; Kumarasamy, E.; Pun, A. B.; Trinh, M. T.; Choi, B.; Xia, J. L.; Taffet, E. J.; Low, J. Z.; Miller, J. R.; Roy, X.; et al. Quantitative Intramolecular Singlet Fission in Bipentacenes. *J. Am. Chem. Soc.* **2015**, *137*, 8965–8972.

(20) Liu, H. Y.; Nichols, V. M.; Shen, L.; Jahansouz, S.; Chen, Y. H.; Hanson, K. M.; Bardeen, C. J.; Li, X. Y. Synthesis and Photophysical Properties of a "Face-To-Face" Stacked Tetracene Dimer. *Phys. Chem. Chem. Phys.* **2015**, *17*, 6523–6531.

(21) Cook, J.; Carey, T. J.; Damrauer, N. H. Solution-Phase Singlet Fission in a Structurally Well-Defined Norbornyl-Bridged Tetracene Dimer. *J. Phys. Chem. A* **2016**, *120*, 4473–4481.

(22) Schrauben, J. N.; Akdag, A.; Wen, J.; Havlas, Z.; Ryerson, J. L.; Smith, M. B.; Michl, J.; Johnson, J. C. Excitation Localization/ Delocalization Isomerism in a Strongly Coupled Covalent Dimer of 1,3-Diphenylisobenzofuran. *J. Phys. Chem. A* **2016**, *120*, 3473–3483.

(23) Korovina, N. V.; Das, S.; Nett, Z.; Feng, X.; Joy, J.; Haiges, R.; Krylov, A. I.; Bradforth, S. E.; Thompson, M. E. Singlet Fission in a Covalently Linked Cofacial Alkynyltetracene Dimer. *J. Am. Chem. Soc.* **2016**, *138*, 617–627.

(24) Zeng, T.; Goel, P. Design of Small Intramolecular Singlet Fission Chromophores: An Azaborine Candidate and General Small Size Effects. *J. Phys. Chem. Lett.* **2016**, *7*, 1351–1358.

(25) Lukman, S.; Chen, K.; Hodgkiss, J. M.; Turban, D. H. P.; Hine, N. D. M.; Dong, S. Q.; Wu, J. S.; Greenham, N. C.; Musser, A. J. Tuning the Role of Charge-Transfer States in Intramolecular Singlet Exciton Fission through Side-Group Engineering. *Nat. Commun.* **2016**, *7*, 13622.

(26) Margulies, E. A.; Miller, C. E.; Wu, Y.; Ma, L.; Schatz, G. C.; Young, R. M.; Wasielewski, M. R. Enabling Singlet Fission by Controlling Intramolecular Charge Transfer in π -Stacked Covalent Terrylenediimide Dimers. *Nat. Chem.* **2016**, *8*, 1120–1125.

(27) Zirzlmeier, J.; Casillas, R.; Reddy, S. R.; Coto, P. B.; Lehnher, D.; Chernick, E. T.; Papadopoulos, I.; Thoss, M.; Tykwienski, R. R.; Guldi, D. M. Solution-Based Intramolecular Singlet Fission in Cross-Conjugated Pentacene Dimers. *Nanoscale* **2016**, *8*, 10113–10123.

(28) Sanders, S. N.; Kumarasamy, E.; Pun, A. B.; Steigerwald, M. L.; Sfeir, M. Y.; Campos, L. M. Intramolecular Singlet Fission in Oligoacene Heterodimers. *Angew. Chem., Int. Ed.* **2016**, *55*, 3373–3377.

(29) Sanders, S. N.; Kumarasamy, E.; Pun, A. B.; Appavoo, K.; Steigerwald, M. L.; Campos, L. M.; Sfeir, M. Y. Exciton Correlations in Intramolecular Singlet Fission. *J. Am. Chem. Soc.* **2016**, *138*, 7289–7297.

(30) Sakuma, T.; Sakai, H.; Araki, Y.; Mori, T.; Wada, T.; Tkachenko, N. V.; Hasobe, T. Long-Lived Triplet Excited States of Bent-Shaped Pentacene Dimers by Intramolecular Singlet Fission. *J. Phys. Chem. A* **2016**, *120*, 1867–1875.

(31) Carey, T. J.; Snyder, J. L.; Miller, E. G.; Sammakia, T.; Damrauer, N. H. Synthesis of Geometrically Well-Defined Covalent Acene Dimers for Mechanistic Exploration of Singlet Fission. *J. Org. Chem.* **2017**, *82*, 4866–4874.

(32) Basel, B. S.; Zirzlmeier, J.; Hetzer, C.; Phelan, B. T.; Krzyaniak, M. D.; Reddy, S. R.; Coto, P. B.; Horwitz, N. E.; Young, R. M.; White, F. J.; et al. Unified Model for Singlet Fission within a Non-Conjugated Covalent Pentacene Dimer. *Nat. Commun.* **2017**, *8*, 15171.

(33) Tayebjee, M. J. Y.; Sanders, S. N.; Kumarasamy, E.; Campos, L. M.; Sfeir, M. Y.; McCamey, D. R. Quintet Multiexciton Dynamics in Singlet Fission. *Nat. Phys.* **2017**, *13*, 182–188.

(34) Kumarasamy, E.; Sanders, S. N.; Tayebjee, M. J. Y.; Asadpoordarvish, A.; Hele, T. J. H.; Fuemmeler, E. G.; Pun, A. B.; Yablon, L. M.; Low, J. Z.; Paley, D. W.; et al. Tuning Singlet Fission in Pi-Bridge-Pi Chromophores. *J. Am. Chem. Soc.* **2017**, *139*, 12488–12494.

(35) Dean, J. C.; Zhang, R.; Hallani, R. K.; Pensack, R. D.; Sanders, S. N.; Oblinsky, D. G.; Parkin, S. R.; Campos, L. M.; Anthony, J. E.; Scholes, G. D. Photophysical Characterization and Time-Resolved Spectroscopy of a Anthradithiophene Dimer: Exploring the Role of Conformation in Singlet Fission. *Phys. Chem. Chem. Phys.* **2017**, *19*, 23162–23175.

(36) Sanders, S. N.; Kumarasamy, E.; Pun, A. B.; Steigerwald, M. L.; Sfeir, M. Y.; Campos, L. M. Singlet Fission in Polypentacene. *Chem. Commun.* **2016**, *1*, 505–511.

(37) Liu, H. Y.; Wang, R.; Shen, L.; Xu, Y. Q.; Xiao, M.; Zhang, C. F.; Li, X. Y. A Covalently Linked Tetracene Trimer: Synthesis and Singlet Exciton Fission Property. *Org. Lett.* **2017**, *19*, 580–583.

(38) Schrauben, J. N.; Zhao, Y. X.; Mercado, C.; Dron, P. I.; Ryerson, J. L.; Michl, J.; Zhu, K.; Johnson, J. C. Photocurrent Enhanced by Singlet Fission in a Dye-Sensitized Solar Cell. *ACS Appl. Mater. Interfaces* **2015**, *7*, 2286–2293.

(39) Dexter, D. L. Two Ideas on Energy-Transfer Phenomena - Ion-Pair Effects Involving the OH Stretching Mode, and Sensitization of Photo-Voltaic Cells. *J. Lumin.* **1979**, *18–19*, 779–784.

(40) Berkelbach, T. C.; Hybertsen, M. S.; Reichman, D. R. Microscopic Theory of Singlet Exciton Fission. II. Application to Pentacene Dimers and the Role of Superexchange. *J. Chem. Phys.* **2013**, *138*, 114103.

(41) Greyson, E. C.; Vura-Weis, J.; Michl, J.; Ratner, M. A. Maximizing Singlet Fission in Organic Dimers: Theoretical Investigation of Triplet Yield in the Regime of Localized Excitation and Fast Coherent Electron Transfer. *J. Phys. Chem. B* **2010**, *114*, 14168–14177.

(42) Grumstrup, E. M.; Johnson, J. C.; Damrauer, N. H. Enhanced Triplet Formation in Polycrystalline Tetracene Films by Femtosecond Optical-Pulse Shaping. *Phys. Rev. Lett.* **2010**, *105*, 257403.

(43) Paddon-Row, M. N.; Patney, H. K. An Efficient Synthetic Strategy for Naphthalene Annellation of Norbornenylogous Systems. *Synthesis* **1986**, *1986*, 328–330.

(44) Scholes, G. D.; Ghiggino, K. P.; Oliver, A. M.; Paddon-Row, M. N. Through-Space and Through-Bond Effects on Exciton Interactions in Rigidly Linked Dinaphthyl Molecules. *J. Am. Chem. Soc.* **1993**, *115*, 4345–4349.

(45) Schwoerer, M.; Wolf, H. C. *Organic Molecular Solids*; Wiley-VCH: Weinheim, 2007.

(46) Johnson, J. C.; Nozik, A. J.; Michl, J. The Role of Chromophore Coupling in Singlet Fission. *Acc. Chem. Res.* **2013**, *46*, 1290–1299.

(47) Spano, F. C. The Spectral Signatures of Frenkel Polarons in H- and J-Aggregates. *Acc. Chem. Res.* **2010**, *43*, 429–439.

(48) Reichardt, C. Solvatochromic Dyes as Solvent Polarity Indicators. *Chem. Rev.* **1994**, *94*, 2319–2358.

(49) Yang, Y.; Davidson, E. R.; Yang, W. T. Nature of Ground and Electronic Excited States of Higher Acenes. *Proc. Natl. Acad. Sci. U. S. A.* **2016**, *113*, E5098–E5107.

(50) Lewis, J. E.; Maroncelli, M. On the (Uninteresting) Dependence of the Absorption and Emission Transition Moments of Coumarin 153 on Solvent. *Chem. Phys. Lett.* **1998**, *282*, 197.

(51) Stern, H. L.; Musser, A. J.; Gelinas, S.; Parkinson, P.; Herz, L. M.; Bruzek, M. J.; Anthony, J.; Friend, R. H.; Walker, B. J. Identification of a Triplet Pair Intermediate in Singlet Exciton Fission in Solution. *Proc. Natl. Acad. Sci. U. S. A.* **2015**, *112*, 7656–7661.

(52) Burgdorff, C.; Ehrhardt, S.; Loehmannsroeben, H. G. Photochemical Properties of Tetracene Derivatives in Solution. 2. Halogenated Tetracene Derivatives. *J. Phys. Chem.* **1991**, *95*, 4246–4249.

(53) Dauben, W. G.; Disanayaka, B.; Funhoff, D. J. H.; Kohler, B. E.; Schilke, D. E.; Zhou, B. L. Polyene 2(1)Ag and 1(1)Bu States and the Photochemistry of Previtamin-D3. *J. Am. Chem. Soc.* **1991**, *113*, 8367–8374.

(54) Fletcher, A. N.; Bliss, D. E. Laser Dye Stability. Part 5. *Appl. Phys.* **1978**, *16*, 289–295.

(55) Van der Auweraer, M.; Grabowski, Z. R.; Rettig, W. Molecular Structure and the Temperature-Dependent Radiative Rates in Twisted Intramolecular Charge-Transfer and Exciplex Systems. *J. Phys. Chem.* **1991**, *95*, 2083–2092.

(56) Weller, A. Photoinduced Electron-Transfer in Solution - Exciplex and Radical Ion-Pair Formation Free Enthalpies and Their Solvent Dependence. *Z. Phys. Chem.* **1982**, *133*, 93–98.

(57) Meylemans, H. A.; Lei, C.-F.; Damrauer, N. H. Ligand Structure, Conformational Dynamics, and Excited-State Electron Delocalization for Control of Photoinduced Electron Transfer Rates in Synthetic Donor-Bridge-Acceptor Systems. *Inorg. Chem.* **2008**, *47*, 4060–4076.

(58) Li, Y.; Zhou, M.; Niu, Y. L.; Guo, Q. J.; Xia, A. D. Solvent-Dependent Intramolecular Charge Transfer Delocalization/Localization in Multibranched Push-Pull Chromophores. *J. Chem. Phys.* **2015**, *143*, 034309.

(59) Carlotti, B.; Benassi, E.; Spalletti, A.; Fortuna, C. G.; Elisei, F.; Barone, V. Photoinduced Symmetry-Breaking Intramolecular Charge Transfer in a Quadrupolar Pyridinium Derivative. *Phys. Chem. Chem. Phys.* **2014**, *16*, 13984–13994.

(60) Terenziani, F.; Painelli, A.; Katan, C.; Charlot, M.; Blanchard-Desce, M. Charge Instability in Quadrupolar Chromophores: Symmetry Breaking and Solvatochromism. *J. Am. Chem. Soc.* **2006**, *128*, 15742–15755.